Author:
Please list all the corrections, indicating page # and line # and e-mail it to Editor at **"sudarshan@compuserve.com" with a copy to "MDSAAB75@giasmd01.vsnl.net.in" within 72 hrs of receipt**

	Editor	Author
Received proof on		
Sent corrected proof on		
Initials		

If you are returning corrected proof as hard copy, please fill in relevant cells.

Paper Ref. #: CR02

Advances in PSII Deposited Diamond-Like Carbon Coatings for Use as a Corrosion Barrier

R. S. Lillard, D. P. Butt, N. P. Baker, K. C. Walter, and M. Nastasi
Materials Science and Technology Division
Los Alamos National Laboratory, P.O. Box 1663, M.S. G755
Los Alamos, NM 87545

Abstract

Plasma source ion implantation (PSII) is a non line of sight process for implanting complex shaped targets without the need for complex fixturing. The breakdown initiation of materials coated with diamond-like carbon (DLC) produced by PSII occurs at defects in the DLC which expose the underlying material. To summarize these findings, a galvanic couple is established between the coating and exposed material at the base of the defect. Pitting and oxidation of the base metal leads to the development of mechanical stress in the coating and eventually spallation of the coating. This paper presents our current progress in attempting to mitigate the breakdown of these coatings by implanting the parent material prior to coating with DLC. Ideally one would like to implant the parent material with chromium or molybdenum which are known to improve corrosion resistance, however, the necessary organometallics needed to implant these materials with PSII are not yet available. Here we report on the effects of carbon, nitrogen, and boron implantation on the susceptibility of PSII-DLC coated mild steel to breakdown.

1.0 Introduction

There currently exists a broad range of applications for which the ability to produce an adherent, hard, wear and, corrosion-resistant coating plays a vital role. These applications include engine components, orthopedic devices, textile manufacturing components, hard disk media, optical coatings, and cutting and machining tools. Plasma-based ion beam processing can play an important role in all of these technologies. The ability to provide flux, energy, and temporal control of a variety of ions, provides an avenue to tailor surface structure and chemistry necessary to solve current and future problems related to corrosion, surface hardness and tribological properties. Ion implantation is a well established ion beam based surface modification technique which has been successfully used to enhance materials engineering performance in areas such as, hardness, friction and wear, fracture toughness, and corrosion.[3-5] Plasma source ion implantation (PSII) developed by J.R Conrad[6-8] at the

Surface Modification Technologies XII
Edited by T.S. Sudarshan, K.A. Khor, and M. Jeandin

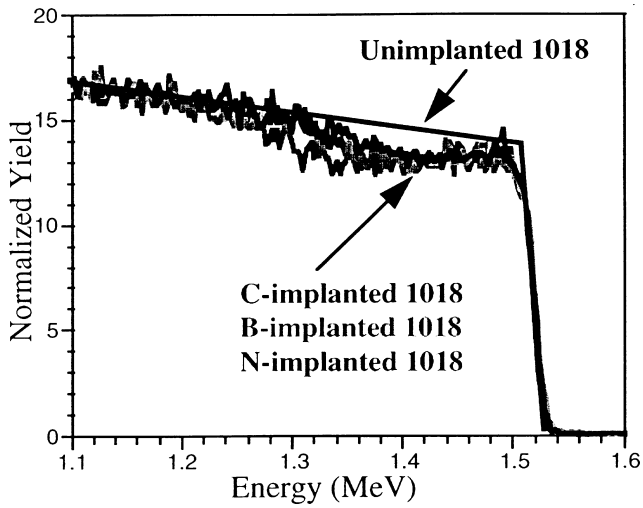

Fig. 1: RBS profiles showing the implantation profiles for B^+, N^+, and C^+ implanted samples. The smooth curve simulates the RBS spectra for unimplanted C1018. The implantation profiles for each ion is inferred from the reduced yield in the RBS spectra in the energy range of 1.26 to 1.53 MeV. A lower yield corresponds to a higher concentration of the implanted ion.

University of Wisconsin is a non-line-of-sight process for implanting complex shaped targets without the need for complex fixturing and, therefore, is a unique method for coating materials to be used in engineering applications.

The breakdown mechanism for PSII diamond like carbon coatings, on CVD nickel[9] has been investigated with electrochemical impedance spectroscopy. Examination in buffer solutions revealed the presence of small defects in the DLC presumably formed in the deposition process. Breakdown of the DLC coating occurred rapidly in chloride solution. However, breakdown failed to initiate in chlorides solution buffered with sodium borate.

It was concluded that the first step in the breakdown mechanism is the preferential dissolution of Ni from the bottom of a pore in the DLC. Although both the Ni dissolution and oxygen reduction reactions may initially occur simultaneously inside the pore, due to restricted diffusion, oxygen is eventually depleted from the pore. Because the boldly exposed DLC is capable of supporting the cathodic reaction and only anodic reactions are taking place in the pore, a galvanic couple is established. To maintain charge neutrality (in the absence of hydroxyl formation), Cl- must migrate into the pore causing the chloride concentration to increase such that the pitting potential of Ni is decreased to that of the couple potential. This formation of a critical propagation solution is considered to be the second step in the breakdown process and must occur to maintain the corrosion reaction, otherwise, the Ni substrate will passivate.

This paper presents our current efforts to mitigate the breakdown of DLC coatings produced by PSII. Specifically, ion implantation of the surface prior to DLC deposition has been evaluated as a method for mitigating breakdown. Ideally one would like to implant the parent material with chrome or molybdenum which are known to improve corrosion resistance, however, the necessary organometallics needed to implant these materials in PSII are not yet available. Here we report on the effects of carbon, nitrogen, and boron implantation on the susceptibility of PSII-DLC coatings to breakdown.

2.0 Experimental

Carbon steel C1018 samples were ground with successively finer grits of SiC followed by polishing with alumina on a polishing wheel. The final polish was 0.3 µm alumina. After polishing, the samples were ultrasonically cleaned in acetone, followed by methanol. After cleaning, some samples were placed in a beamline ion implantation chamber and implanted with either B^+, N^+, or C^+ at 35 keV. Boron ions were generated by flowing CCl_4 gas over boron powder at 600°C. Gaseous boron-chlorine compounds are formed and used to generate the $11B^+$ beam. Nitrogen and carbon ions were generated from N_2 and CO_2 gases, respectively. The implantation produced near surface concentration profiles as seen in Figure 1. The retained ion doses were 3.1, 1.2, and 2.0 x 10^{17} at·cm^{-2} respectively for B, N, and C. While these elements were chosen because of the ability to form secondary phases with iron, no heat treatment was employed to form these phases. In addition, no attempt was made to identify their presence. Other C1018 samples were placed in a PSII chamber and sputter-cleaned with Ar ions, implanted with carbon ions from a methane plasma, and Ar sputter-cleaned again to remove any carbon deposit resulting from the implantation process. DLC was then deposited onto this surface from an RF plasma of acetylene (4.5 mTorr total pressure). The final DLC thickness was approximately 4 to 5 µm.[10] Transmission electron microscopy of similar specimens have shown the DLC structure to be amorphous.[11] The DLC coating had a density of 1.9 g·cm-3 and consisted of approximately 70 at% C and 30 at% hydrogen

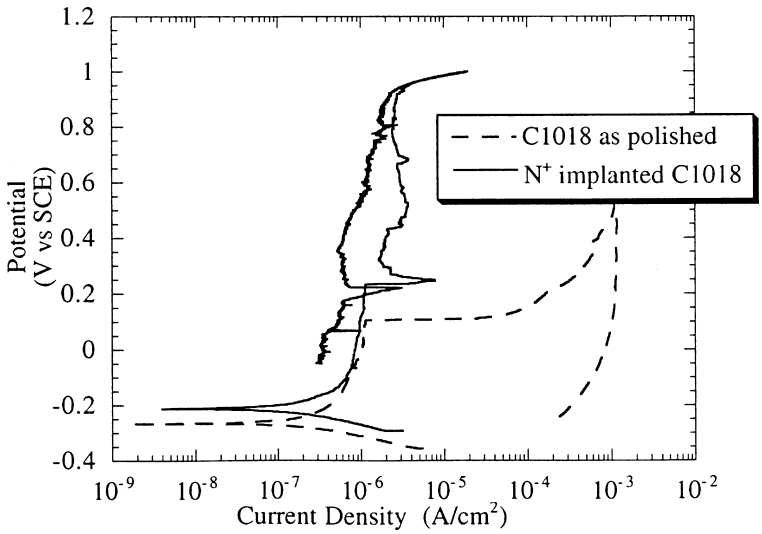

Fig. 2: Potentiodynamic polarization curves for as polished and N^+ implanted C1018 steel in borate buffered 0.005 M NaCl (pH 8.2).

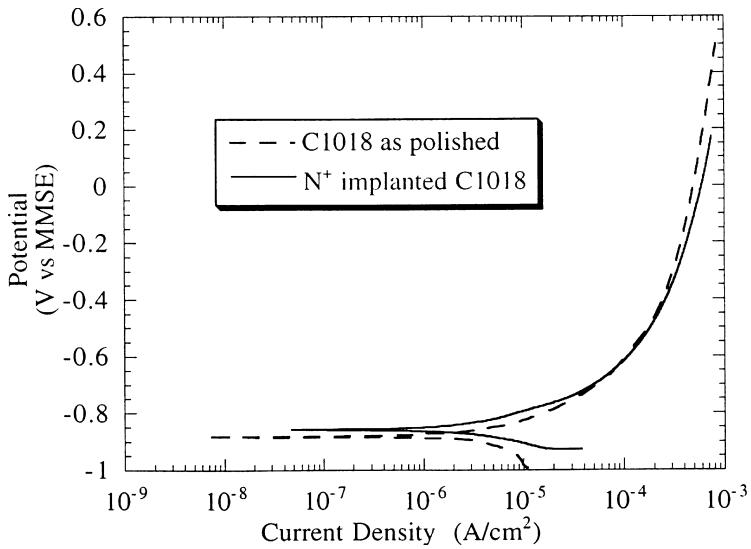

Fig. 3: Potentiodynamic polarization curves for as polished and N^+ implanted C1018 steel in 0.001 M sodium sulfate pH 8.2.

(H). The C:H ratio was found to greatly effect coating properties with lower hydrogen content yielding coatings with the highest hardness values. The C:H ratio also effected coating resistivity and adhesion. The hardness of the DLC coatings examined was found to be to directly proportional to sp^3 content. The DLC coating had a hardness of about 12 GPa and an sp^3 content of ~20%.

Electrochemical experiments were conducted in 0.15 molar (M) boric acid / 0.0375 M sodium borate pH 8.2, 0.15 M boric acid / 0.0375 M sodium borate / 0.005 M sodium chloride pH 8.2, 0.001 M sodium sulfate pH 8.2, and ASTM artificial ocean water pH 8.2. Potentiodynamic polarization curves were run at a scan rate of 0.2 $mV \cdot s^{-1}$. Electrochemical impedance spectroscopy (EIS) measurements were performed at the open circuit potential over the frequency range of $1x10^{-3}$ to $1x10^4$ Hz. To eliminate chloride contamination, a mercury / mercury sulfate reference electrode (MMSE; +0.640 V vs. normal hydrogen electrode (NHE)) was used with non-chloride containing solutions. In chloride containing solutions a saturated calomel electrode (SCE, +0.241 vs. NHE) was used. For the sake of clarity, all potentials are referenced vs SCE.

3.0 Results and Discussions

3.1 Effects of N^+, C^+, and B^+ Implantation

Typical potentiodynamic polarization curves for N^+ implanted C1018 in 0.005 M NaCl / borate buffer solution and 0.001 Na_2SO_4 are presented in Figures 2 and 3 respectively. As seen in Figure 2 no pitting potential for the N^+ implanted

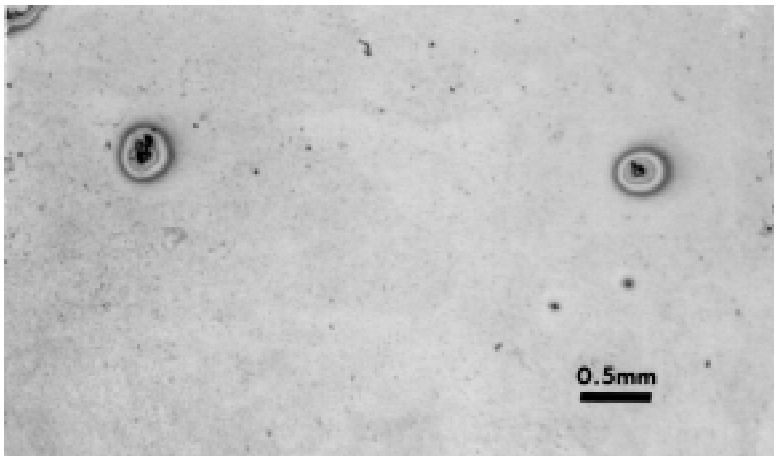

Fig. 4: Optical micrograph of a typical corrosion pit found in N^+ implanted C1018 steel after potentiodynamic polarization of the sample above the pitting potential. The concentric rings around the pit are believed to be corrosion product.

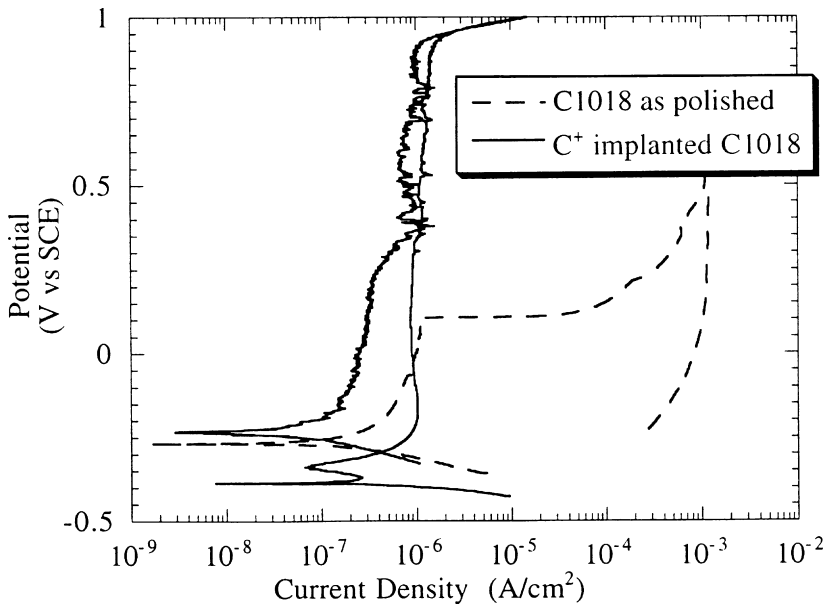

Fig. 5: Potentiodynamic polarization curves for as polished and C^+ implanted C1018 steel in borate buffered 0.005 M NaCl (pH 8.2).

sample in Cl^- solution was observed. Moreover, no positive hysterysis during the reverse scan was observed indicating active pitting of the sample was not occurring above the OCP. However, some small corrosion pits were observed in the surface of the N^+ implanted sample after the polarization experiment as seen in Figure 4. This is an indication that N+ implantation does not effect initiation but rather, propagation. In Na_2SO_4 solution active dissolution was observed for both the implanted and as polished samples at all applied anodic potentials. Similar results were obtained for C^+ implanted C1018 samples as seen in Figures 5.

Typical potentiodynamic polarization curves for B^+ implanted and as polished C1018 in 0.005M NaCl / borate buffer solution are presented in Figure 6. As seen in this Figure B^+ implantation offers no improved corrosion resistance in Cl- solution. To the contrary, at all applied anodic potentials active dissolution of the B^+ implanted sample was observed.

3.2 Corrosion of C^+ Implanted C1018 Coated with DLC

Bode magnitude phase plots for C1018 steel implanted with C^+ and then coated with DLC are presented in Figures 7. The solution used for these experiments was ASTM artificial seawater. As can be seen in this figure, three time constant appear in the EIS data. The equivalent circuit EC used to model this behavior is presented in Figure 8. This EC differs somewhat from earlier models.[6] In this system the intrinsic electrical properties of the DLC layer are represented by the elements C^i_{DLC} and R^i_{DLC} where the superscript 'i' represents

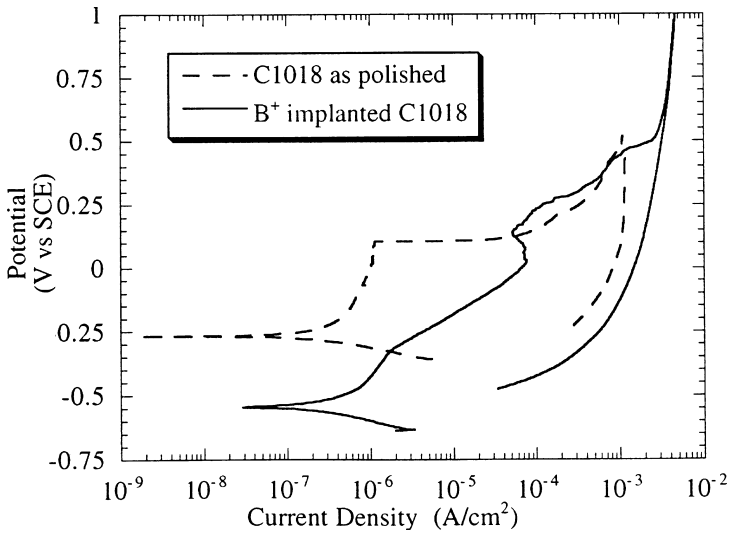

Fig. 6: Potentiodynamic polarization curves for as polished and B^+ implanted C1018 steel in borate buffered 0.005 M NaCl (pH 8.2).

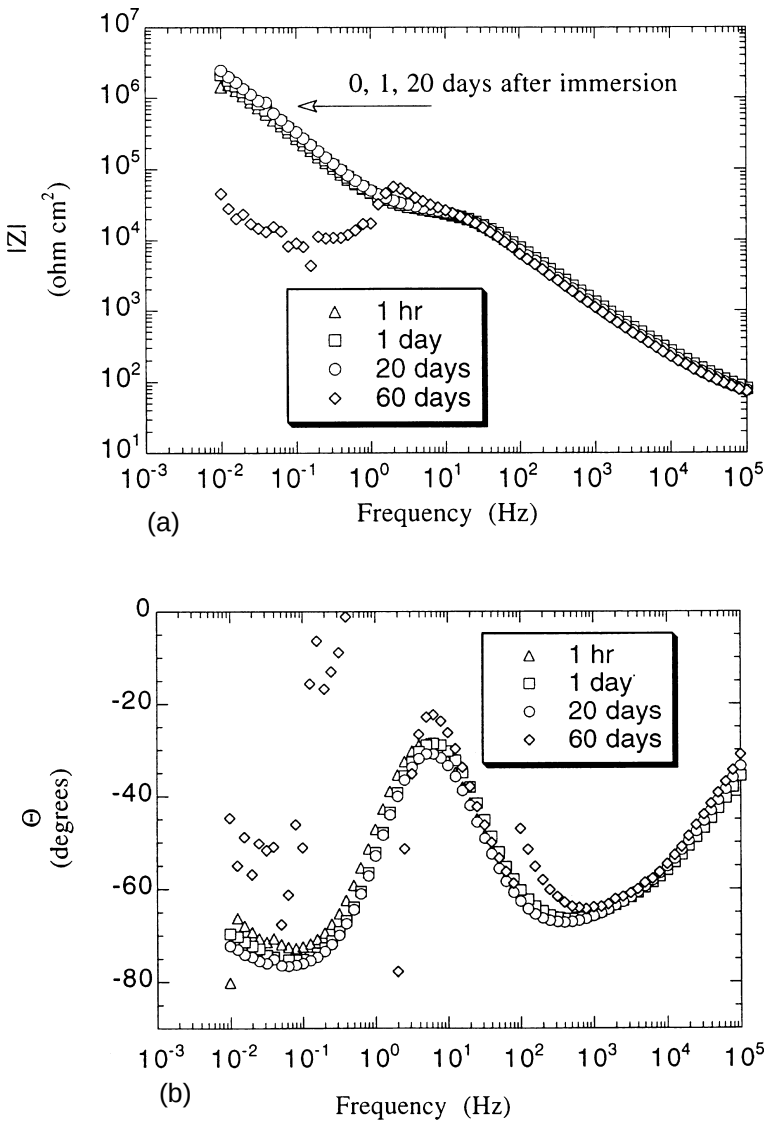

Fig. 7: (a) Bode magnitude and (b) Bode phase plots for DLC coated C1018 steel in ASTM artificial seawater as a function of immersion time. Note that the C1018 sample was implanted with C^+ prior to coating with DLC.

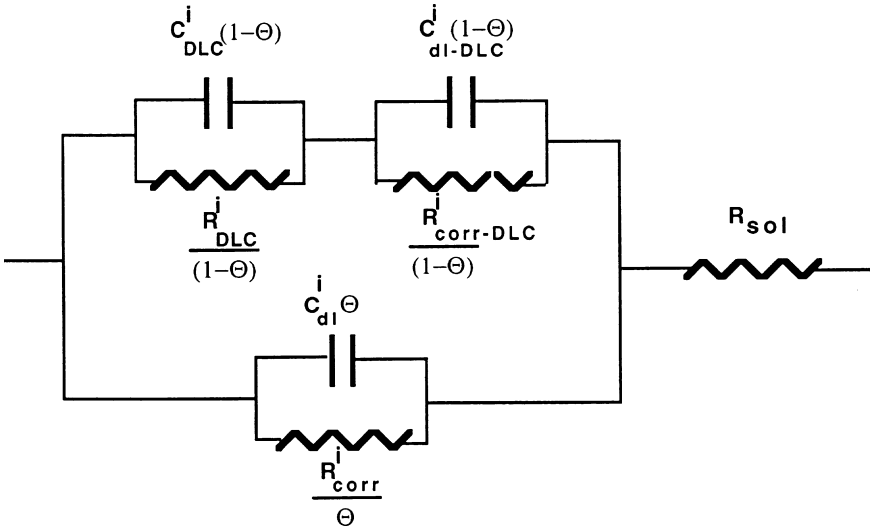

Fig. 8: Equivalent circuit used to model the EIS data where: C^i_{DLC} and R^i_{DLC} represent the intrinsic electrical properties of the DLC layer, C^i_{CR} and R^i_{CR} represent the capacitance and charge transfer resistance of the DLC, C^i_{dl} and R^i_{corr} double layer capacitance, and Θ represents the fraction of surface covered by these pinholes.

''intrinsic''. This layer acts in series with the charge transfer reaction occurring at the DLC/solution interface represented by the elements C^i_{DLC} and R^i_{DLC} which model the capacitance and charge transfer resistance of the DLC. The elements representing the DLC layer and DLC act in parallel with small ''pinholes'' in the DLC (less than 20 μm in diameter). These pinholes expose either the carbon implanted layer, a very thin DLC layer or, a combination of both. As will be shown later in this paper, these pinholes act as initiation sites for breakdown and are, therefore, associated with a double layer capacitance and corrosion resistance, C^i_{dl} and R^i_{corr} respectively. The fraction of surface covered by these pinholes is defined by Θ and the fraction of surface covered by DLC is defined by 1-Θ. The observed (measured with EIS) parameters will necessarily scale with Θ. These 'observed' elements are represented by a superscript 'o'. For example: $R^0_{corr} = R^0_{corr} / \Theta$ and $R^0_{DLC} = R^i_{DLC}/(1-\Theta)$.

As seen in Figure 7 little change in the EIS data was observed for the first 20 days of immersion. In comparison, the breakdown of DLC coated CVD Ni in a solution with lower Cl^- concentration occurred in only 24 hrs. Unfortunately, the relative lifetime of C^+ implanted DLC coated steel is still short for engineering applications. As seen in Figure 7, after 60 days of immersion a dramatic decrease in the low frequency data was observed. In addition, the EIS response after 60 days clearly does not fit the EC model presented in Figure 8. After removal from solution the sample was covered with copious amounts of corrosion product. Moreover the DLC was flaking off of the steel substrate as in filiform corrosion.

4.0 Summary

The effects of C^+, N^+, and B^+ implantation into C1018 steel to mitigate the breakdown of DLC coating has been investigated. Both C^+ and N^+ implanted C1018 steel (as implanted, no coating) showed marked improvement in the susceptibility to pitting corrosion while B^+ implantation displayed active dissolution at all anodic potentials. Although as polished C1018 steel had a pitting potential of approximately 0.11 V SCE, no pitting potential was observed in C^+ and N^+ implanted samples. Moreover, no positive hysteresis in the anodic polarization curves for C^+ and N^+ implanted samples was observed indicating that pit propagation was not occurring. However, a few small pits were observed in the implanted samples after potentiodynamic polarization indicating that C^+ and N^+ implantation does not effect initiation but rather, propagation.

The breakdown of C^+ implanted C1018 steel coated with DLC in ASTM artificial seawater was investigated with EIS. In comparison to DLC coated Ni samples, breakdown was delayed. However, the relative lifetime of C^+ implanted DLC coated steel is still short for engineering applications. After 60 days of immersion a dramatic decrease in the low frequency data was observed. After removing the sample from solution the sample was covered with copious amounts of corrosion product. Moreover the DLC was flaking off of the steel substrate as in filaform corrosion.

5.0 Acknowledgments

Work on this project was performed under the auspices of the University of California for the U.S. Department of Energy contract W-7405-ENG-36. N.P. Baker, K.C. Walter, and M. Nastasi are funded by the DOE office of Basic Energy Science.

6.0 References

1. J. Robertson, Progress in Solid State Chemistry, **21**(1), 1991, p.199.

2. K.C. Walter, M. Nastasi, H. Kung, P. Kodali, C. Munson, I. Henins, and B.P. Wood, Diamond-Like Carbon Deposition for Tribological Applications at Los Alamos National Laboratory, *Materials Research Society Symposium Proceedings*, **383**, 1995.
3. A.H. Al-Saffar, V. Ashworth, A.K.O. Bairamov, D.J. Chivers, W.A. Grant, and R.P.M. Procter, *Corrosion Science*, **20**(1), 1980, p.127.
4. V. Ashworth, R.P.M. Procter, and W.A. Grant, *Application of Ion Implantation to Aqueous Corrosion, in Ion Implantation*, J.K. Hirvonen, ed., Academic Press, New York, 1980.
5. P.M. Natishan, E. McCafferty, and G.K. Hubler, *Journal of the Electrochemical Society*, **135**(2), 1987, p.321.
6. J.R. Conrad, Materials Science and Engineering A-Structural Materials Properties Microstructure and Processing, **116**(197), 1989.
7. M. Madapura, J.R. Conrad F.J. Worzala, R.A. Dodd, F.C. Prenger, and J.A. Barclay, *Surface and Coatings Technology*, **39**(1-3) 1989, p.587.
8. J.T. Scheuer, M. Shamim, and J.R. Conrad, *Journal of Applied Physics*, **67**(3), 1990, p.1241.
9. R.S. Lillard, D.P. Butt, T.N. Taylor, K.C. Walter, and M. Nastasi, *Corrosion Science*, **39**(9), 1997, p.1605.
10. D.P. Butt, K.C. Walter, M. Nastasi, A.L. Campuzano, P.S. Martin, B.P. Wood, D.J. Rej, and G.G. Miller, *Philosophical Magazine Letters*, **70**(6) 1994, p.385
11. M. Nastasi, J.P. Hivonen, G.M. Pharr, and W.C. Oliver, *Journal of Materials Research*, **3**(2) 1988, p.226.
12. ASTM D 1161, 1987 Annual Book of ASTM Standards, ASTM, Philadelphia, PA, 1987.

Author:

Need page numbers for Refs. 2, 4, and 6

Editor